JOURNAL OF SOLID STATE CHEMISTRY 72, 181–192 (1988)

Crystal Structure of the $\beta BaZr_2F_{10}$ Compound. Relations with the ReO_3-type and the Fluorozirconate Glasses

J. P. LAVAL AND B. FRIT[1]

Laboratoire de Chimie Minérale Structurale, UA–CNRS No. 320, Université de Limoges, 123, avenue A. Thomas, 87060 Limoges Cedex, France

AND J. LUCAS

Laboratoire de Chimie Minérale D, UA–CNRS No. 254, Université de Rennes I, Campus de Beaulieu, avenue du Général Leclerc, 35042 Rennes Cedex, France

Received December 23, 1986; and in revised form March 27, 1987

The high temperature $\beta BaZr_2F_{10}$ phase crystallizes with triclinic symmetry and unit-cell parameters a = 24.256(9) Å, b = 15.383(6) Å, c = 9.057(3) Å, α = 90.00°(7), β = 112.98°(7), γ = 90.57°(5) (space group $P1$ or $P\bar{1}$, Z = 16). In fact, this triclinic cell is a one-dimensional supercell ($a \times 4$) of a basic pseudomonoclinic subcell with $C2/c$ or Cc possible space groups. With this monoclinic subcell, an average structure (space group $C2/c$) has been solved and refined to a conventional R = 0.056 for 411 independent reflections. The structure consists of a three-dimensional network of corner- and/or edge-sharing ZrF_7 and BaF_{11} anionic polyhedra. It can also be described either as a regular succession along 0y of identical $BaZr_2F_{17}$ polyhedral layers sharing horizontal and oblique edges, or as a 2D network of interpenetrated zig-zag chains of ZrF_7 pentagonal bipyramids, joined together by twisted Ba sheets. Structural relations with the ReO_3 type and with the corresponding fluorozirconate glasses are considered.

I. Introduction

Since their first discovery in the binary system BaF_2–ZrF_4 (*1*) and in other various ternary BaF_2–MF_n–ZrF_4 systems (*2*), the ZrF_4-based glasses have received increasing attention, due to their high technological interest (*3*). However, the knowledge of their structure, absolutely essential for a good understanding—and then a mastery—of their properties, is far from being perfect since numerous different models, often contradictory, have been proposed (*4–13*).

Just now, the lack of long-range order prevents any possibility of a direct interpretation of experimental data provided by modern techniques; so, the short-range order determination requires the prior elaboration of structural models to be compared with these experimental data.

The crystalline phases with composition

[1] To whom correspondence should be addressed.

0022-4596/88 $3.00

TABLE I

CRYSTALLOGRAPHIC CHARACTERISTICS OF THE α AND $\beta BaZr_2F_{10}$ PHASES

		$\beta BaZr_2F_{10}$	
		True cell (superstructure)	Reduced cell (subcell)
Symmetry	$\alpha BaZr_2F_{10}$ Triclinic	Triclinic	Monoclinic
Unit-cell parameters			
a (Å)	13.013(5)	4 × 6.064(2)	6.064
b (Å)	7.794(3)	15.383(6)	15.383
c (Å)	17.452(6)	9.057(3)	9.057
α (°)	93.13(7)	90.00(7)	90
β (°)	118.20(7)	112.98(7)	112.98
γ (°)	92.10(7)	90.57(7)	90
Space group	$P\bar{1}$, $P1$	$P1$, $P\bar{1}$	$C2/c$; Cc
d_{exp}	4.32 ± 0.05	4.33 ± 0.05	
d_{calc}	4.35	4.35	
z	8	16	4

close to those of the glasses, or formed during the crystallization of these glasses, are undoubtedly the best source of information for the elaboration of such models. For example, an accurate analysis of the crystal structure of αZrF_4 (*14*) and of both α and $\beta BaZrF_6$ (*15, 16*) allowed a significant improvement of the structural knowledge of BaF_2–ZrF_4 glasses (compositional range: 50–75 mole% ZrF_4) (*5–7*).

Our investigations within the BaF_2–ZrF_4 system (*17*) allowed us to synthesize and characterize, in addition to both α and $\beta BaZrF_6$ polymorphs and other numerous stoichiometric and nonstoichiometric phases, the $BaZr_2F_{10}$ compound. This latter is dimorphic and exhibits a reversible $\alpha \rightleftarrows \beta$ transition at 460°C. At that time, the poor quality of the crystals discouraged us from undertaking the crystal structure determination of these two phases. Since then, numerous crystallization studies of fluorozirconate glasses have quasisystematically shown the formation of $\beta BaZr_2F_{10}$ crystals (*18–27*). So, the knowledge of the crystal structure of this phase has become vital and in spite of unfavorable technical conditions, we undertook its determination.

The crystallographic characteristics of $\beta BaZr_2F_{10}$ as well as the $\alpha BaZr_2F_{10}$ ones, are reported in Table I.

All the XRD patterns show clearly that the true triclinic cell is a one-dimensional supercell ($a \times 4$) of a basic pseudomonoclinic subcell with $C2/c$ or Cc space group. Because of the subcell predominance and of the small size of the available crystals, the number of supercell reflections accurately measurable, was extremely low. Hence, we found a full structure analysis unrealistic and we have proceeded to a determination of an average structure with the monoclinic subcell and the most symmetrical $C2/c$ spacegroup.

II. Structure Determination

The selected crystal had a nearly spherical shape. 1088 diffracted intensities were collected on a Nonius CAD-3 automated diffractometer (MoK_α radiation, graphite monochromator, $\theta-2\theta$ scan with $4° \leq \theta \leq 35°$). Because of the small size of the crystal ($\langle R \rangle \simeq 0.025$ mm) no absorption corrections had to be made ($\mu R = 0.2$). After averaging equivalent (or more exactly pseudoequivalent) reflections and correcting for Lorentz-polarization effects, 411 independent intensities such as $I \geq 2.2\sigma(I)$, were available for the structure determination with the SHELX-76 computing program (*22*). The scattering factors for Ba, Zr, and F atoms were those reported in "International Tables for X-ray Crystallography" (*23*). They have been corrected for anomalous dispersion effects.

The heavy atoms Ba and Zr have been located from the three-dimensional Patterson function. With these data, a Fourier-difference synthesis allowed the determination of the coordinates of fluorine atoms.

Refinements involving the coordinates and the isotropic thermal factors of all the atoms led then to a satisfactory value for the reliability factor: $R = 0.075$. However, successive Fourier-difference maps exhibited electron density anomalies located in the neighborhood of the cationic sites, especially the zirconium ones. Although not negligible, they were not strong enough to justify a splitting of the corresponding positions. We have tried to eliminate them by introducing anisotropic thermal coefficients for the Zr atom. The best results ($R = 0.056$) have been obtained by taking into account the thermal anisotropy of only the Zr atoms (Table II). It can be seen that, apart from the Ba atoms, the statistical superposition in an "average reduced cell" of crystallographically nonequivalent atoms leads to an important, but artificial, increase of their thermal factors. However, it is reasonable to think that the given values are not very different from the true ones and give a good idea of the real structure, the superstructure and the triclinic deformation being only a consequence of slight atomic displacements. Indeed the corresponding interatomic distances (Table III) do not exhibit any important anomalies.

TABLE II

COORDINATES AND THERMAL COEFFICIENTS OF THE DIFFERENT ATOMS IN THE $\beta BaZr_2F_{10}$ CRYSTAL STRUCTURE

Atom	Position	x	y	z	B_{iso} B_{eq} (Zr)[a] (Å^2)
Ba	4*e*	0	0.1729(2)	1/4	1.30(5)
Zr	8*f*	0.1700(5)	0.4057(2)	0.1013(3)	1.79(8)
F(1)	8*f*	0.333(2)	0.046(1)	0.431(2)	1.6(2)
F(2)	4*e*	0	0.445(2)	1/4	2.4(4)
F(3)	4*e*	0	0.951(2)	1/4	4.8(6)
F(4)	8*f*	0.221(3)	0.112(1)	0.070(2)	3.5(4)
F(5)	8*f*	0.450(4)	0.197(2)	0.517(3)	5.9(6)
F(6)	8*f*	0.283(4)	0.312(2)	0.257(3)	5.9(5)

[a] For the Zr atom, the anisotropic coefficients are: $\beta_{11} = 0.036(1)$, $\beta_{22} = 0.018(1)$, $\beta_{33} = 0.014(1)$, $\beta_{12} = 0.007(1)$, $\beta_{13} = 0.013(1)$, $\beta_{23} = 0.016(1)$.

TABLE III

INTERATOMIC DISTANCES (Å) WITHIN THE BaF_{11} AND ZrF_7 POLYHEDRA AND SHORTEST CATION–CATION DISTANCES

Ba_1–$F(1)_1$ = 2.83(1)	Zr_1–$F(1)_1$ = 2.16(1)	Ba_1–Zr_1 = 4.243(3)
Ba_1–$F(3)_1$ = 3.41(3)	Zr_1–$F(1)_2$ = 2.17(1)	Ba_1–Zr_3 = 4.534(4)
Ba_1–$F(4)_1$ = 2.65(2)	Zr_1–$F(2)_1$ = 2.08(1)	Ba_1–Zr_4 = 4.097(3)
Ba_1–$F(5)_1$ = 2.84(2)	Zr_1–$F(3)_2$ = 2.05(1)	Ba_1–Zr_5 = 4.540(4)
Ba_1–$F(5)_2$ = 2.87(2)	Zr_1–$F(4)_3$ = 1.93(1)	Zr_1–Zr_2 = 3.980(5)
Ba_1–$F(6)_1$ = 2.73(2)	Zr_1–$F(5)_1$ = 2.02(1)	Zr_1–Zr_5 = 3.617(5)
	Zr_1–$F(6)_3$ = 1.95(2)	Zr_2–Zr_3 = 3.854(5)
		Zr_3–Zr_4 = 5.352(6)
⟨Ba–F⟩ = 2.78	⟨Zr–F⟩ = 2.05	Ba_1–Ba_2 = 4.960(2)

About Zr	About Ba
$F(1)_1$–$F(1)_2$ = 2.38(3)	$F(1)_1$–$F(3)_1$ = 2.51(2)
$F(1)_1$–$F(2)_1$ = 2.67(3)	$F(1)_1$–$F(4)_1$ = 3.23(2)
$F(1)_1$–$F(4)_3$ = 2.89(3)	$F(1)_1$–$F(4)_2$ = 3.51(3)
$F(1)_1$–$F(5)_1$ = 2.47(3)	$F(1)_1$–$F(5)_1$ = 2.47(3)
$F(1)_2$–$F(2)_1$ = 2.72(3)	$F(3)_1$–$F(4)_1$ = 3.50(3)
$F(1)_2$–$F(3)_2$ = 2.51(2)	$F(4)_1$–$F(5)_2$ = 3.31(3)
$F(1)_2$–$F(4)_3$ = 2.93(2)	$F(4)_1$–$F(6)_1$ = 3.46(3)
$F(2)_1$–$F(3)_2$ = 3.03(3)	$F(5)_1$–$F(5)_2$ = 2.83(5)
$F(2)_1$–$F(5)_1$ = 2.97(3)	$F(5)_1$–$F(6)_1$ = 2.79(3)
$F(2)_1$–$F(6)_3$ = 2.66(3)	$F(5)_2$–$F(6)_1$ = 2.91(3)
$F(3)_2$–$F(4)_3$ = 2.85(2)	$F(5)_2$–$F(6)_2$ = 2.33(3)
$F(3)_2$–$F(6)_3$ = 2.52(3)	
$F(4)_3$–$F(5)_1$ = 2.75(3)	
$F(4)_3$–$F(6)_3$ = 3.18(3)	
$F(5)_1$–$F(6)_3$ = 2.33(3)	

[a] Notations for atoms are those used in Fig. 2.

III. Description of the Structure

The unit-cell atomic content is shown, projected onto the (010) plane, in Fig. 1. The $\beta BaZr_2F_{10}$ structure is a three-dimensional network of corner- and/or edge-sharing ZrF_7 and BaF_{11} anionic polyhedra in the respective proportion 2–1. However, it also can be described as a regular succession along [010] of identical layers parallel to (010). One of these layers, corresponding to cations with $y \simeq 0.09, 0.17$ is shown in Fig. 2.

1. Anionic Polyhedra (see Fig. 2 and Table III)

The Zr anionic polyhedron is a slightly distorted pentagonal bipyramid with $F(1)_1$, $F(5)_1$, $F(6)_3$, $F(3)_2$, $F(1)_2$ atoms as equatorial corners and $F(2)_1$, $F(4)_3$ atoms as axial

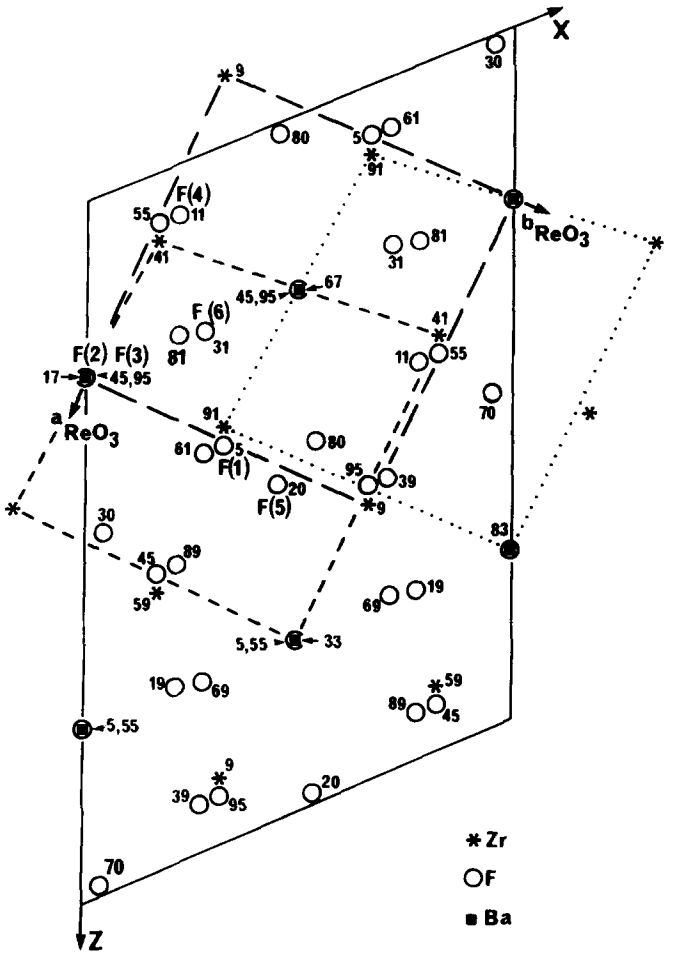

FIG. 1. Projection (010) of the $\beta BaZr_2F_{10}$ unit-cell content. Three successive cationic 4^4 subcells are represented by dotted or dashed lines.

ones. The Zr–F distances range from 1.93 to 2.17 Å, but the average distance ⟨Zr–F⟩ = 2.05 Å is quite comparable with the usually observed values for sevenfold coordinated zirconium (2.02–2.08 Å) (*4*). This polyhedron can be also described as an octahedron with one corner replaced by a $F(5)_1$–$F(6)_3$ edge.

The more complex BaF_{11} ployhedron can be considered as an irregular square antiprism whose two triangular faces ($F(5)_3$–$F(1)_3$–$F(6)_2$ and $F(5)_2$–$F(1)_1$–$F(6)_1$ in Fig. 2) and a square one ($F(1)_3$–$F(4)_1$–$F(1)_1$–$F(4)_2$ in Fig. 2) are each capped by an extra anion (respectively, $F(5)_4$, $F(5)_1$, and $F(3)_1$ in Fig. 2). However, the Ba–$F(3)_1$ distance is much longer than the other ones (Ba–$F(3)_1$) = 3.41 Å for an average ⟨Ba–F⟩ = 2.78 Å), and the true Ba coordination must be considered as [10 + 1].

2. Polyhedra Distribution in the (010) Planes

In the polyhedral layers parallel to (010), the cations are distributed in a [Ba–Zr–Zr] sequence along quasi-orthogonal [$\bar{1}$01] and

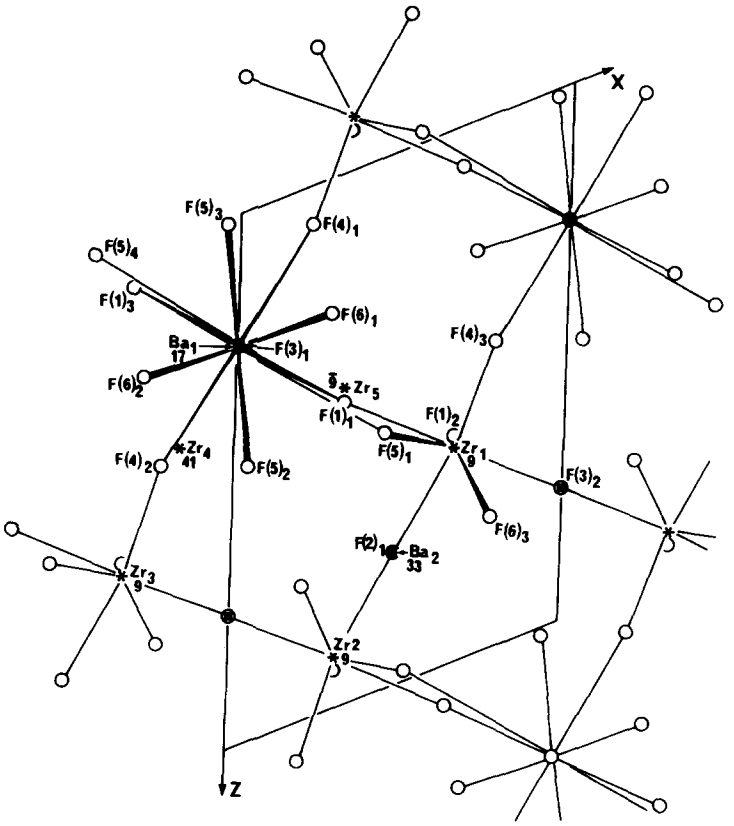

FIG. 2. A $BaZr_2F_{17}$ layer of BaF_{11} and ZrF_7 polyhedra.

[201] rows, so constituting a square 4^4 network: this network is not perfectly planar since the Ba atoms (with $y = 0.17$ for instance in Fig. 2) are shifted 1.2 Å out of the Zr atom plane ($y = 0.09$ in Fig. 2). In each layer, the polyhedra share only corners along [$\bar{1}$01] and alternately corners and edges along [201]. In this way, each ZrF_7 polyhedron is bound to two identical polyhedra by corner-sharing, to one BaF_{11} polyhedron by edge-sharing and to one other BaF_{11} polyhedron by corner-sharing, and each BaF_{11} polyhedron is bound to four ZrF_7 polyhedra, two by corner-sharing, two by edge-sharing. Logically each edge-sharing leads to a noticeable shortening of the Ba–Zr distance (4.24 Å instead of 4.53 Å for a corner-sharing bond).

3. *Interlayer Bonding*

The identical polyhedral layers stack another along [010] in such a way that the cationic 4^4 subcells are not superposed but alternatively translated (see Fig. 1). If we take the original layer as the one with cations at $y = 0.09$ and 0.17, the upper layer, i.e., the one with cations at $y = 0.33$, 0.41, is shifted by a $\frac{1}{8}\mathbf{n}_{10\bar{1}}$ vector. The lower layer, the one with cations at $y = -0.09$ and -0.17, is shifted by a $\frac{1}{8}\mathbf{n}_{201}$ vector.

As a consequence, in each layer, the BaF_{11} polyhedra are linked on one side to two BaF_{11} polyhedra by sharing in each case an oblique F(5)–F(5) edge ($d Ba_1$–Ba_2 = 4.96 Å) and to two ZrF_7 polyhedra by sharing parallel and horizontal F(5)–F(6)

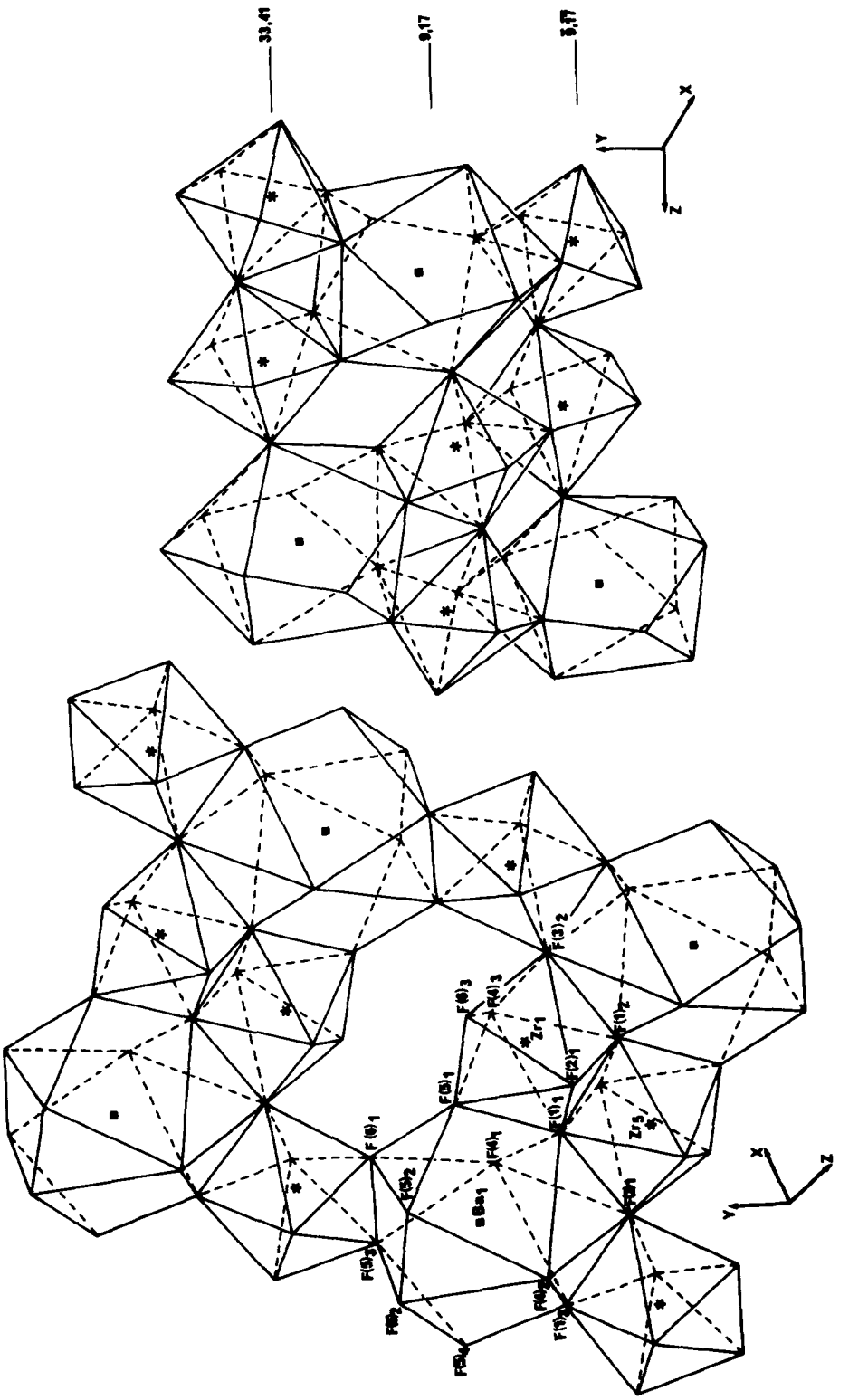

FIG. 3. Two perspective views of the 3D linking of BaF_{11} and ZrF_7 polyhedra.

edges (dBa_1–Zr_4 = 4.10 Å). On the opposite side the BaF_{11} polyhedra are linked to two other ZrF_7 polyhedra (in the staggered position relative to the former ones) by sharing F(1)–F(3) oblique edges (dBa_1–Zr_5 = 4.54 Å). The ZrF_7 polyhedra are linked on one side to a BaF_{11} polyhedron by sharing an horizontal F(5)–F(6) edge and on the opposite side both to another ZrF_7 polyhedron by sharing an oblique F(1)–F(1) edge (dZr_1–Zr_5 = 3.62 Å) and to a BaF_{11} polyhedron by sharing an oblique F(1)–F(3) edge. Figure 3 gives perspective views of the layer packing along 0*y* and of the 3D linking of polyhedra.

IV. Structural Relations with ReO_3-Type Structures

As illustrated in Fig. 4, each polyhedral layer of the $\beta BaZr_2F_{10}$ structure, formula $BaZr_2F_{17}$ ($MX_{5.67}$), can be obtained from an ideal $BaZr_2F_{12}$ (MX_4) layer of corner-sharing BaF_6 and ZrF_6 octahedra, characteristic of the ReO_3 structure, by a one-sided substitution of the free octahedral corners by either a square face for the BaF_6 octahedra or an edge for the ZrF_6 octahedra. Such a substitution, in fact, replaces one of the two less dense 4^4 anionic subcells (formula *X* for one MX_3 formula unit) of the ReO_3 structure, by a slightly folded much more dense 3^34^2 subcell ($MX_{2.67}$ formula) composed with the F(5) and F(6) anions at y = 0.19, 0.20, 0.30, and 0.31 (see Fig. 2).

The change from the 3D network of corner-sharing MX_6 octahedra, characteristic of the ReO_3 structure, to the $\beta BaZr_2F_{10}$ 3D network of corner and/or edge-sharing ZrX_7 and BaX_{11} polyhedra, can be described in a formal way, by the following shear process, illustrated in Fig. 5 and involving three adjacent octahedra layers: (1) a central layer, as for instance the layer with cations at *y* = 0.09 and 0.17, (2) a lower layer translated by $(\frac{1}{2}\mathbf{n}_{011})_{ReO_3}$, which changes the common corners into oblique common edges and removes the purely anionic 4^4 subcell (formula *X*), and (3) an upper layer translated by $(\frac{1}{2}\mathbf{n}_{100})_{ReO_3}$, then removal of the BaX_6 free octahedral corners and substitution of edges parallel to $[010]_{ReO_3}$ for the ZrX_6 free corners, leading to a compaction of the anionic subcell from *X* to $X_{2.67}$ (3^34^2 anionic subcell).

The . . . MX_2–*X*–MX_2–*X* . . . stacking sequence characteristic of the ReO_3 structure is now replaced by the . . . MX_2–MX_2–$X_{2.67}$ . . . stacking sequence observed in $\beta BaZr_2F_{10}$. Because of the large difference in size of Ba^{2+} and Zr^{4+} cations, such a process is only possible with a strictly ordered distribution of cations and with an important distortion of the anionic and cationic subcells within the ReO_3-type polyhedral layers. These distortions are actually observed in the βBZr_2F_{10} structure. They correspond in the main to a folding of the anionic planes, all the more important as these planes are dense, and to a shifting of Ba^{2+} and Zr^{4+} cations (indicated by arrows in Figs. 4 and 5) out of the ReO_3-basis plane (mean anionic plane) toward, respectively, the edges and square faces substituted for the original corners. This latter phenomenon, which is absolutely essential to the regularity of cation coordination polyhedra, is a common feature of all the known compounds derived from the ReO_3 type by the creation (ordered or not) of an anion excess, either directly (i.e., with preservation of the cationic cubic subcell) or indirectly (i.e., by a crystallographic shear process).

As shown by the values reported in Table IV the displacement of cations out of the basic plane is all the more important as the cation size is large, and for a given cation the number of anions substituted for the original corner is high and the cationic cubic subcell is more distorted (crystallographic shear planes between ReO_3 layers).

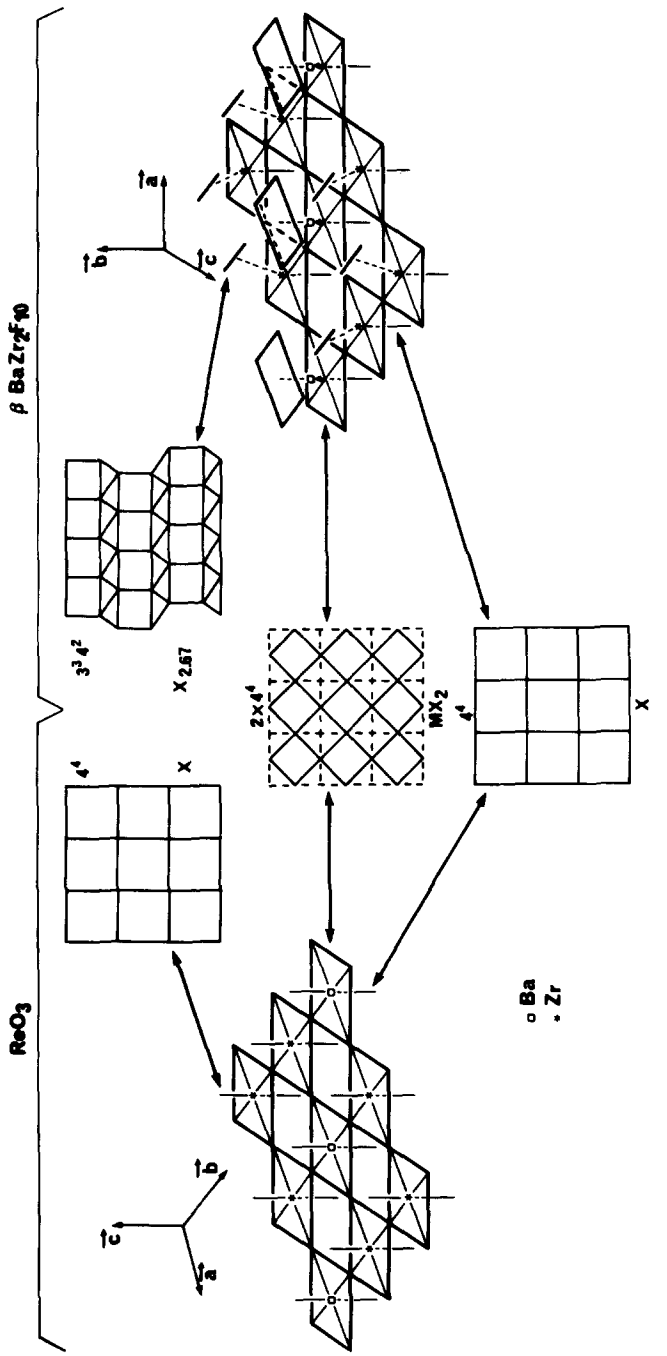

FIG. 4. Comparison of a $BaZr_2F_{12}$ layer (ReO_3 type) with a $BaZr_2F_{17}$ layer ($\beta BaZr_2F_{10}$ type).

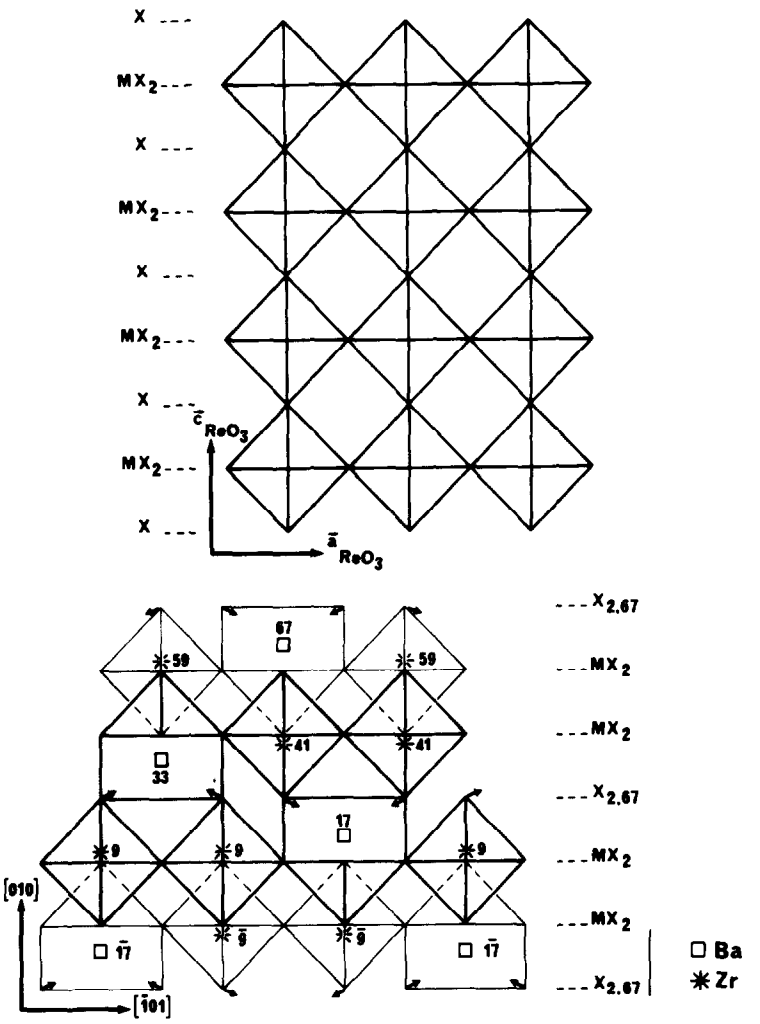

FIG. 5. Transformation by a double shear process of the 3D network of corner-sharing octahedra characteristic of the ReO_3 type into the 3D network of corner- and/or edge-sharing BaF_{11} and ZrF_7 polyhedra characteristic of the $\beta BaZr_2F_{10}$ crystal structure. Coordinates of cations are y ones.

V. Structural Relations with the Fluorozirconate Glasses

For fluorozirconate glasses with chemical compositions equal or close to $BaZr_2F_{10}$, molecular dynamic calculations (*7, 24, 25*) have suggested the presence of ZrF_7 or ZrF_8 units and Angell has shown the particular stability of edge-sharing ZrF_7–ZrF_8 units, even in the molten state (*7*). Actually EXAFS data are in agreement with seven- or eightfold coordinated Zr^{4+} cations (*26*). In addition recent X-ray diffusion experiments (*4, 7*) have revealed the presence, on radial electron distribution curves, of a 3.6-Å peak, interpreted by Lucas (*7*) as characteristic of a

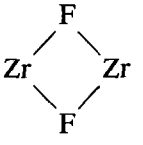

TABLE IV

OBSERVED CATION SHIFTS Δ OUT OF THE ReO_3 BASIC PLANE IN SOME ANION-EXCESS ReO_3-RELATED STRUCTURES

Phases (Ref.)	Cationic Subcell	Part substituted for the octahedron corner	Δ (Å)
$Zr(F,O)_{3.33}$ (*27*)	Cubic	Edge	0.20
$Zr_{0.8}Yb_{0.2}F_{3.2}O_{0.3}$ (*28*)	Cubic	Edge	0.27
	CS		
$SmZrF_7$ (*29*)	$(\frac{1}{2}\mathbf{a}_{100})_{ReO_3}$	Triangular face	Sm → 0.7
	Double *CS*		
$\beta BaZr_2F_{10}$	$(\frac{1}{2}\mathbf{a}_{011})_{ReO_3}$	Edge	Zr → 0.31
	$(\frac{1}{2}\mathbf{a}_{100})_{ReO_3}$	Square face	Ba → 1.54
Ba_2ZrF_8 (*30*)	Cubic	Triangular face	Zr → 0.7 Ba → 1.88

bridge with a very short Zr–Zr distance as in the αZrF_4 structure (*15*).

These results strongly suggest that the crystal structure of $\beta BaZr_2F_{10}$ is probably very close to the corresponding glass structure. So we have tried to extract parts of this structure that could be preserved, more or less distorted, in the glassy state. With increasing complexity we can distinguish the following units.

First Unit

The basic unit of the $\beta BaZr_2F_{10}$ structure is undoubtedly the Zr_2F_{12} association of two edge-sharing ZrF_7 polyhedra. This very stable unit which associates two very close Zr^{4+} cations (d_{Zr-Zr} = 3.62 Å) linked by a

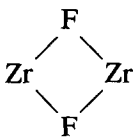

bridge with long Zr–F bonds (2.16 and 2.17 Å) is also present in the $\alpha BaZrF_6$ and the αZrF_4 polymorphs and probably as proposed by Lucas (*7*), in the related glasses.

Second Unit

The Zr_2F_{12} basic units join together by corner-sharing to form infinite zig-zag chains of ZrF_7 pentagonal bipyramids involving Zr atoms from two successive $BaZr_2F_{17}$ layers (e.g., Zr at y = 0.009 and y = −0.09).

Two different kinds of chains can be distinguished. The first ones, schematically shown in Fig. 6a, are parallel to [$\bar{1}$01] ($\mathbf{a}_{ReO_3}$) and are characterized by successive 3.62 Å (edge-sharing) and 3.98 Å (corner-sharing) Zr–Zr distances. The second ones, which are probably more stable since they associate Zr_2F_{12} units by a shorter corner-shared Zr–Zr distance (3.85 Å), are parallel to [201] ($\mathbf{b}_{ReO_3}$) and are shown in Fig. 6b.

Third Unit

In fact, the two kinds of zig-zag chains are interpenetrated and form a 2D network, i.e., a Zr_2F_{10} double layer of corner- and edge-sharing ZrF_7 pentagonal bipyramids. These double layers are linked to each other along [010] through the intermediary of twisted Ba sheets (e.g., Ba atoms at y = 0.17, 0.33 for double layers with Zr atoms at, respectively, y = −0.09, 0.09 and y = 0.41, 0.59 as one can see in Figs. 3 and 5).

Glassy $BaZr_2F_{10}$ is an isotropic material in which it has been proved that a given Zr atom is surrounded by one Zr at a short distance of 3.6 Å and three other Zr atoms at 4.15 Å. By comparison, in $\beta BaZr_2F_{10}$, one Zr atom has three Zr neighbors: one

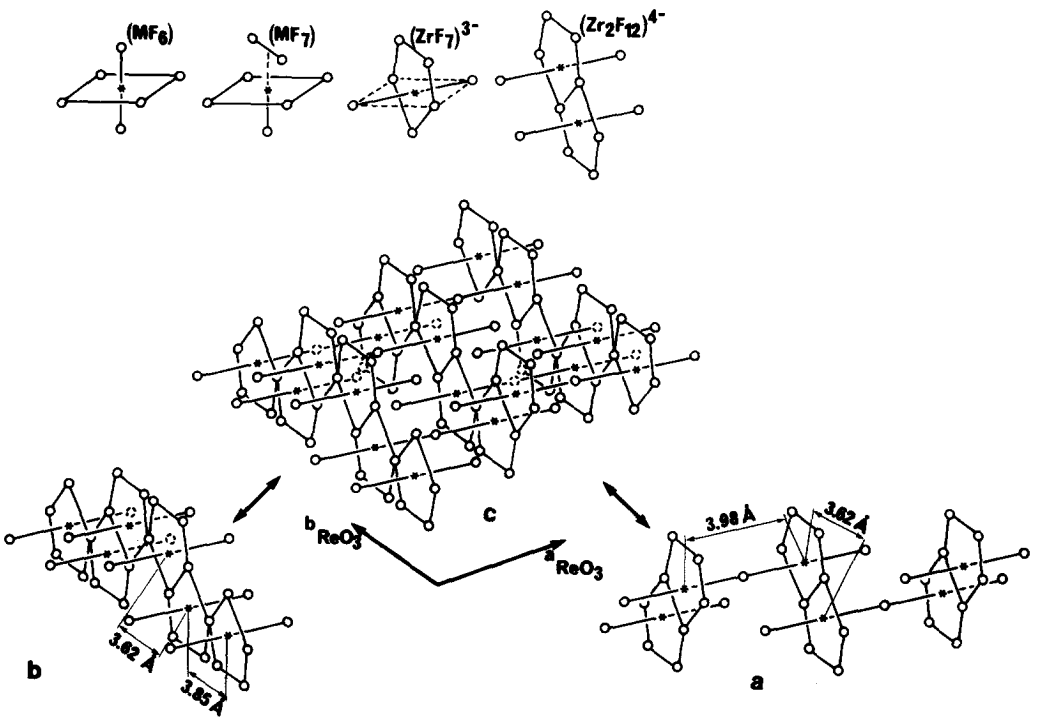

FIG. 6. A double layer of ZrF_7 pentagonal bipyramids (c) resulting from the interpenetration of zig-zag chains parallel to [$\bar{1}$01] (a) and [201] (b). The picture in the left upper corner shows the transformation of a ZrF_6 octahedron into a ZrF_7 pentagonal bipyramid by substituting an edge for a corner.

(edge-sharing) located at 3.62 Å and two other (corner-sharing) located at 3.98 and 3.85 Å.

It is clear that the glass-crystal competition can be explained by the transformation of the 2D character of the $(Zr_2F_{10})^{2-}$ giant anion in the crystal to a 3D network in the glass due to the connection of the double layers through a mechanism which involves the formation of new Zr–F–Zr bonds. This network, due to the complexity and flexibility of the various connections, can exist without any periodicity; the Ba^{2+} ions are statistically distributed within the vitreous lattice. Differential thermal analysis experiments indicate that this vitreous form of $BaZr_2F_{10}$ is highly thermodynamically unstable and tends to rearrange into a crystalline form dominated by strong ionic interactions between the $(Zr_2F_{10})^{2-}$ double layers and the intervening distorted sheets of Ba^{2+} ions.

Conclusion

Though derived from the ReO_3-type by a compacting shear process, the $\beta BaZr_2F_{10}$ 3D network of BaF_{11} and ZrF_7 polyhedra however remains relatively "open," as can be seen in Fig. 3. The strong units of the ZrF_7 pentagonal bipyramids layers can surely be preserved in the glassy state, linked by Ba atoms in a more compact way than in the crystalline state, so justifying the higher densities surprisingly observed in this glassy state ($d BaZr_2F_{10}$ (glass) $\simeq$ 4.5–4.6, $d BaZr_2F_{10}$ (crystal) = 4.35).

References

1. M. POULAIN, M. POULAIN, AND J. LUCAS, *Rev. Chim. Mineral.* **16,** 267 (1979).
2. M. POULAIN, M. POULAIN, J. LUCAS, AND P. BRUN, *Mater. Res. Bull.* **10,** 212 (1975).
3. For a review, see: Halide glasses, *Mater. Sci. Forum* **5–6** (1985).
4. R. COUPE, D. LOUER, J. LUCAS, AND A. J. LEONARD, *J. Amer. Ceram. Soc.* **66,** 523 (1983).
5. Y. KAWAMOTO AND T. HORISAKA, *J. Non-cryst. Solids* **56,** 39 (1983).
6. Y. KAWAMOTO AND F. SAKAGUCHI, *Bull. Chem. Soc. Japan* **56,** 2138 (1983).
7. J. LUCAS, C. A. ANGELL, AND S. TAMADDON, *Mater. Res. Bull.* **19,** 945 (1984).
8. J. LUCAS, D. LOUER, AND C. A. ANGELL, *Mater. Sci. Forum* **6,** 449 (1985).
9. R. M. ALMEDIA AND J. D. MACKENZIE, *J. Chem. Phys.* **74,** 5954 (1981).
10. J. P. LAVAL, B. FRIT, AND J. LUCAS, *Mater. Sci. Forum* **6,** 457 (1985).
11. R. M. ALMEIDA, J. LAU, AND J. D. MACKENZIE, *Mater. Sci. Forum* **19,** 465 (1985).
12. G. COURBION, J. GUERY, A. LE BAIL, AND C. JACOBONI, *Mater. Sci. Forum* **19,** 739 (1985).
13. G. E. WALRAFEN, M. S. HOKMABADI, S. GUHA, P. N. KRISHNAN, AND D. C. TRAN, *J. Chem. Phys.* **83**(9), 4427 (1985).
14. R. PAPIERNIK, D. MERCURIO, AND B. FRIT, *Acta Crystallogr. B* **38,** 2347 (1982).
15. J. P. LAVAL, R. PAPIERNIK, AND B. FRIT, *Acta Crystallogr. B* **34,** 1070 (1978).
16. B. MEHLHORN AND R. HOPPE, *Z. Anorg. Allg. Chem.* **425,** 180 (1976).
17. J. P. LAVAL, B. FRIT, AND B. GAUDREAU, *Rev. Chim. Mineral.* **16,** 509 (1979).
18. N. P. BANSAL, R. H. DOREMUS, A. J. BRUCE, AND C. T. MOYNIHAN, *Mater. Res. Bull.* **19,** 577 (1984).
19. G. F. NEILSON, G. L. SMITH, AND M. C. WEINBERG, *Mater. Res. Bull.* **19,** 279 (1984).
20. W. J. MINISCALCO, L. J. ANDREWS, B. T. HALL, AND D. E. GUENTHER, *Mater. Sci. Forum* **5,** 279 (1985).
21. J. M. PARKER, A. G. CLARE, AND A. B. SEDDON, *Mater. Sci. Forum* **5,** 257 (1985).
22. G. M. SHELDRICK, "SHELX 76, Program for crystal structure determination," Cambridge University (1976).
23. "International Tables for X-ray Cristallography," Vols. II and IV, Kynoch Press, Birmingham (1968).
24. I. YASUI AND H. INOUE, *J. Non-cryst. Solids* **71,** 39 (1985).
25. H. INOUE, H. HASEGAWA, AND I. YASUI, *Phys. Chem. Glasses* **26**(3), 74 (1985).
26. B. BOULARD, A. LE BAIL, J. P. LAVAL, AND C. JACOBONI, "Internat. Conf. on EXAFS, Fontevraud, France, 1986."
27. R. PAPIERNIK AND B. FRIT, *Mater. Res. Bull.* **19,** 509 (1984).
28. B. C. TOFIELD, M. POULAIN, AND J. LUCAS, *J. Solid State Chem.* **27,** 163 (1979).
29. M. POULAIN, M. POULAIN, AND J. LUCAS, *J. Solid State Chem.* **8,** 132 (1973).
30. J. P. LAVAL AND B. FRIT, *Acta Crystallogr. B* **36**(11), 2533 (1980).